NASA TN D-1780

TECHNICAL NOTE

D-1780

GEOMETRICAL CHARACTERISTICS OF LUNAR ORBITS

ESTABLISHED FROM EARTH-MOON TRAJECTORIES

By Robert H. Tolson

Langley Research Center
Langley Station, Hampton, Va.

Code-1

NATIONAL AERONAUTICS AND SPACE ADMINISTRATION

TECHNICAL NOTE D-1780

GEOMETRICAL CHARACTERISTICS OF LUNAR ORBITS

ESTABLISHED FROM EARTH-MOON TRAJECTORIES

By Robert H. Tolson

SUMMARY

/ 5 2 36

An analysis has been made of the geometrical characteristics of lunar orbits which can be established from typical earth-moon transfer trajectories. An iterated two-body or patched-conic technique was used to relate the transfer-trajectory injection conditions to the selenocentric orbital parameters through a set of simultaneous transcendental equations. Solutions to these equations are presented for typical sets of injection conditions. These solutions suggest an additional simplification in the analysis which results in a simple physical understanding of the problem and also in some approximate, simple relationships between the lunar orbital parameters and the transfer-trajectory characteristics.

In particular, it is shown that (unless changes in the orbital plane are instituted) there is a minimum-inclination lunar orbit which can be established. The value of this minimum inclination is given as a function of the injection conditions and depends primarily on the injection flight-path angle and transfer-trajectory inclination to the earth-moon plane. In addition, an approximate equation is given which relates the lunar orbital inclination and nodal position to the injection conditions; hence, only one of these two lunar orbital parameters can be chosen arbitrarily.

INTRODUCTION

Current plans for manned lunar missions include the establishment of a close lunar orbit as a prerequisite to the lunar landing operation; in particular, the establishment of a lunar orbit is an integral part of the lunar orbit rendezvous technique. These plans have stimulated an interest in the types of lunar orbits which can be established efficiently and which at the same time are consistent with the overall mission requirements. For example, suppose a lunar orbit is established prior to landing and that the exploration vehicle lands nearly in this orbital plane, then the question of possible landing sites is closely related to the geometrical characteristics of the permissible lunar orbits.

Of particular interest from the mission-requirement standpoint is the initiation of a satisfactory earth-return trajectory. It is shown in reference 1 that the achievement of such a trajectory, if initiated from a lunar orbit, is

strongly dependent on the geometrical characteristics of that lunar orbit. In fact, for an arbitrary lunar orbit, there may be periods during the month when the return flight cannot be initiated unless costly orbital plane changes are instituted. Hence, if the lunar orbit rendezvous technique is utilized, the lunar orbit must be established such that after the proper exploration time the geometrical characteristics of the orbit are within the allowable band for satisfactory, efficient return to earth.

An analysis was initiated at the NASA Langley Research Center to investigate the geometrical characteristics of lunar orbits which can be established to be consistent with typical constraints on the earth-to-moon transfer trajectory. A "patched-conic" technique was used to relate the lunar orbital parameters to the transfer-trajectory parameters through a set of transcendental equations. Some solutions to these equations are presented for typical transfer trajectories. These solutions motivate a further approximation which leads to a simpler set of equations and a better physical understanding of the problem.

SYMBOLS

$\bar{D}$ vector distance from center of earth to center of moon

$\bar{e}_x, \bar{e}_y, \bar{e}_z$ unit vectors along X-, Y-, and Z-axes, respectively

$\bar{h}$ geocentric angular momentum vector

i inclination of selenocentric orbital plane to earth-moon plane

i_o inclination of transfer-trajectory plane to earth-moon plane

l_1, m_1, n_1 direction cosines between x_m and X-, Y-, and Z-axes, respectively

l_2, m_2, n_2 direction cosines between y_m and X-, Y-, and Z-axes, respectively

$\bar{r}$ geocentric position vector of vehicle at the sphere of influence

r_o geocentric injection radius

$\bar{R}$ selenocentric position vector of vehicle at the sphere of influence

R_p periselenian distance of selenocentric hyperbola

$\bar{V}_e$ geocentric velocity vector of vehicle

$\bar{V}_m$ geocentric velocity vector of the moon

$\bar{V}_s$ selenocentric velocity vector of vehicle at the sphere of influence

2

$\left(\dfrac{V}{V_p}\right)_o$ ratio of injection velocity to parabolic velocity at the injection altitude

x, y, z geocentric position components

$\dot{x}, \dot{y}, \dot{z}$ geocentric velocity components

x_m, y_m selenocentric position components measured in the selenocentric orbital plane

α nondimensional radius of the sphere of influence, $R/D = 0.1498$

β acute angle between $\overline{R}$ and $\overline{V}_S$

γ_o injection flight-path angle

η latitude of entry point on sphere of influence

θ angular position in selenocentric orbital plane

λ nondimensional velocity, V_S/V_m

$\mu = \cos \eta \sin \xi$

μ_e gravitational constant of the earth

μ_m gravitational constant of the moon

τ approximate flight time from earth injection to periselenian point

$\nu = \cos \eta \cos \xi$

ξ angular position of entry point on the sphere of influence

Ω longitude of node of selenocentric orbital plane

Ω_o longitude of node of transfer-trajectory plane

Subscripts:

x, y, z components along X-, Y-, and Z-axes, respectively

n   normal impact selenocentric trajectory

c   center of locus of entry points

min   minimum

ANALYSIS AND DISCUSSION

The characteristics of lunar orbits are directly dependent on the characteristics of the earth-to-moon transfer trajectory from which they are established. Hence, constraints imposed on the transfer trajectory by mission requirements will limit the types of lunar orbits which can be established efficiently, that is, established without orbital transfers or plane changes. It would be convenient to have explicit relationships between the earth-injection parameters and the lunar orbital elements so that the effects of these limitations might be investigated; unfortunately, no exact analytical expressions have been found. Numerical integration of the equations of motion of a vehicle in cislunar space do not readily yield any general indications of these relationships; however, these studies show that the lunar orbital characteristics can be changed appreciably by making small changes in the transfer trajectory and thus a wide variety of lunar orbits can be established from essentially the same earth-to-moon trajectory.

Some approximations are required in order to obtain general analytical information about the relations between the transfer-trajectory characteristics and the lunar orbital characteristics. In this study, the earth and moon are assumed to move in circular orbits at the mean distance of 238,857 miles and in addition a patched-conic technique is utilized with a lunar sphere of influence as defined in reference 2. While the vehicle is inside the imaginary selenocentric sphere, the earth's gravitational effects on the vehicle are neglected and when the vehicle is outside the sphere the moon's gravity is neglected. As illustrated in figure 1, the motion is represented by two conic sections, the first
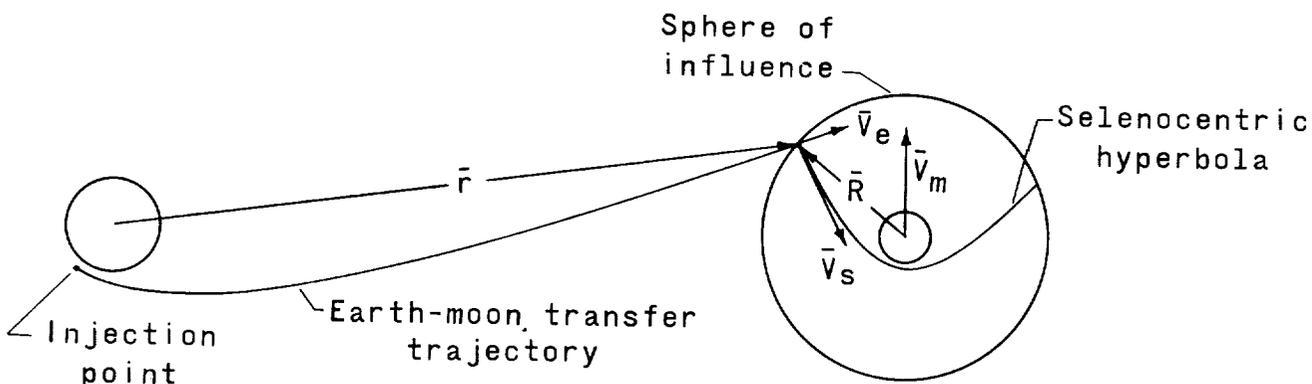

Figure 1.- Illustration of patched-conic technique.

geocentric and the second selenocentric, which are "patched" at the sphere of influence to make the trajectory continuous. The utility of the above assumptions is that they reduce the problem from one defined by a system of differential equations to one defined by a set of transcendental equations. The solutions to the latter equations are readily obtained by an iterative technique.

The patched-conic technique relates the characteristics of the transfer trajectory to the characteristics of the selenocentric approach hyperbola; however, for the most efficient establishment of a lunar orbit, the lunar orbital plane should coincide with the plane of the selenocentric hyperbola, and as indicated in reference 3, the orbit should be established when the vehicle is near periselenian and such that the periselenian point of the resulting lunar orbit nearly coincides with the periselenian point of the approach hyperbola. Under these conditions, the geometrical characteristics (inclination, nodal position, and altitude at periselenian) of the lunar orbit are the same as the characteristics of the selenocentric hyperbola from which the orbit is established; therefore, a study of the geometry of the approach hyperbola is equivalent to studying the geometry of the resulting lunar orbit.

General Equations and Solution

In a patched-conic technique the geocentric $\left(\bar{r}, \ \overline{V}_e\right)$ and selenocentric $\left(\overline{R}, \ \overline{V}_s\right)$ position and velocity vectors at the sphere of influence are expressed in terms of the respective orbital parameters. Then to insure that the trajectory is continuous across the sphere of influence, the position and velocity vectors are related by $\bar{r} = \overline{R} + \overline{D}$ and $\overline{V}_e = \overline{V}_s + \overline{V}_m$. These equations give the required number of relationships so that the selenocentric orbital elements can be determined from the geocentric orbital elements. By utilizing these equations, the position of the entry point (i.e., the point where the vehicle passes through the sphere of influence) relative to the earth can be given in terms of the position relative to the moon by

$$
\left.
\begin{aligned}
x &= Rl_1 + D \\[2mm]
y &= Rm_1 \\[2mm]
z &= Rn_1
\end{aligned}
\right\}
\tag{1}
$$

where, as indicated in figure 2, the coordinate system is chosen with the origin at the earth's center, the X-axis points in the direction of the moon at the time the vehicle passes through the sphere of influence, and the Z-axis is normal to the earth-moon plane.

The velocity components at the entry point are related by

$$
\left.
\begin{aligned}
\dot{x} &= V_s\left(l_2 \sin \beta - l_1 \cos \beta\right) \\[2mm]
\dot{y} &= V_s\left(m_2 \sin \beta - m_1 \cos \beta\right) + V_m \\[2mm]
\dot{z} &= V_s\left(n_2 \sin \beta - n_1 \cos \beta\right)
\end{aligned}
\right\}
\tag{2}
$$

where β is the acute angle between $\overline{R}$ and $\overline{V}_s$ and where the direction cosines are expressed in terms of the angles illustrated in figure 2

5
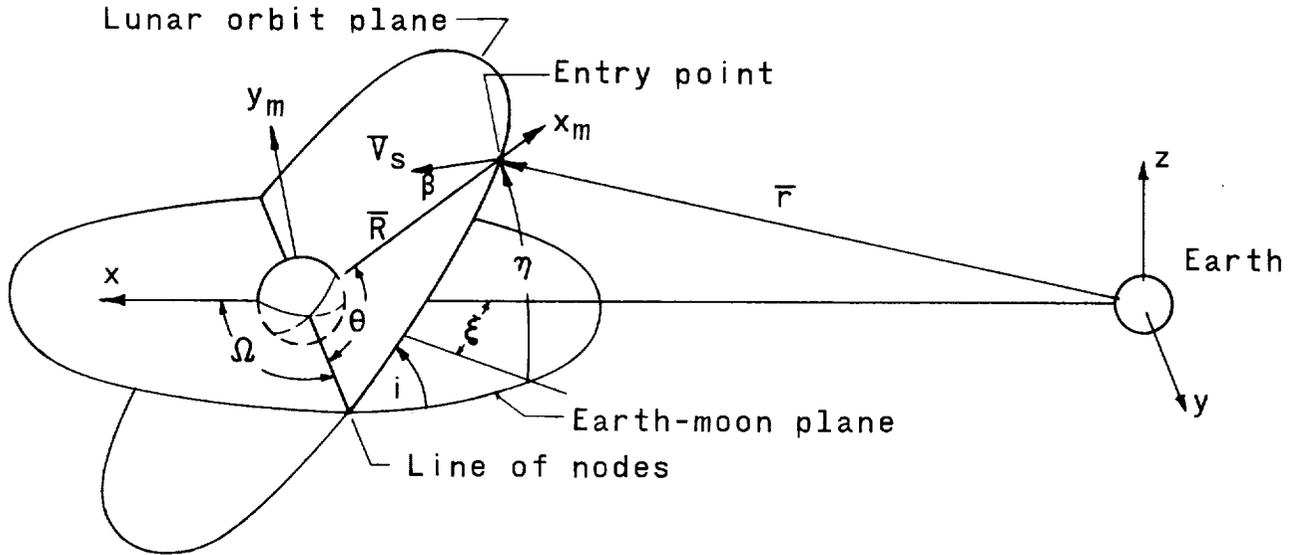
Figure 2.- Illustration of coordinate system and angular parameters.

$$l_1 = \cos\theta \cos\Omega - \sin\theta \sin\Omega \cos i$$

$$l_2 = -\sin\theta \cos\Omega - \cos\theta \sin\Omega \cos i$$

$$m_1 = \cos\theta \sin\Omega + \sin\theta \cos\Omega \cos i$$

$$m_2 = -\sin\theta \sin\Omega + \cos\theta \cos\Omega \cos i$$

$$n_1 = \sin\theta \sin i$$

$$n_2 = \cos\theta \sin i$$

The geocentric velocity and position vectors of the vehicle at the sphere of influence are related to the transfer-trajectory injection conditions through the laws of conservation of energy and angular momentum; namely,

$$\left.\begin{array}{l} \dfrac{2\mu_e}{r_o}\left[\left(\dfrac{V}{V_p}\right)_o^2 - 1\right] = \left(\dot{x}^2 + \dot{y}^2 + \dot{z}^2\right) - 2\mu_e\left(x^2 + y^2 + z^2\right)^{-1/2} \\[2ex] h_x = h \sin i_o \sin\Omega_o = y\dot{z} - z\dot{y} \\[2ex] h_y = -h \sin i_o \cos\Omega_o = z\dot{x} - x\dot{z} \\[2ex] h_z = h \cos i_o = x\dot{y} - y\dot{x} \end{array}\right\} \qquad (3)$$

6

where the total geocentric angular momentum is given by

$$h = \sqrt{2\mu_e r_0} \left(\frac{V}{V_p}\right)_0 \cos \gamma_0$$

The inclination i_0 and the nodal position Ω_0 of the transfer-trajectory plane are measured relative to the coordinate system in figure 2 and in a manner directly analogous to i and Ω for the lunar orbital plane. Substituting equations (1) and (2) into the right-hand side of equations (3) gives the selenocentric orbital parameters (V_s, θ, Ω, i, β) on the right in terms of the transfer-trajectory parameters $\left(\gamma_0,\ r_0,\ \left(\frac{V}{V_p}\right)_0,\ i_0,\ \Omega_0\right)$ on the left; explicitly,

$$\frac{2\mu_e}{r_0}\left[\left(\frac{V}{V_p}\right)_0^2 - 1\right] = V_s^2 + V_m^2 - 2V_sV_m(m_1 \cos \beta - m_2 \sin \beta)$$

$$- \frac{2\mu_e}{D}\left[1 + \left(\frac{R}{D}\right)^2 + 2\left(\frac{R}{D}\right)\ell_1\right]^{-1/2}$$

$$h \sin i_0 \sin \Omega_0 = (RV_s \sin \beta \sin \Omega - RV_m \sin \theta)\sin i$$

$$h \sin i_0 \cos \Omega_0 = \left[RV_s \sin \beta \cos \Omega - DV_s \sin(\theta - \beta)\right] \sin i$$

$$h \cos i_0 = -DV_s\left[\cos(\theta - \beta)\sin \Omega + \sin(\theta - \beta)\cos \Omega \cos i\right] + RV_s \sin \beta \cos i$$

$$+ DV_m + RV_m\left[\cos \theta \cos \Omega - \sin \theta \sin \Omega \cos i\right]$$

For manned lunar missions it is generally required that the selenocentric hyperbola have a specified periselenian distance, R_p. This condition provides a relationship between V_s and β obtained from the conservation of energy and angular momentum relative to the moon; namely,

$$\sin \beta = \left(\frac{R_p}{R}\right)\sqrt{1 + \frac{2\mu_m}{R_p V_s^2}\left(1 - \frac{R_p}{R}\right)} \tag{4}$$

7

Hence, by assuming that R_p is fixed, equations (3) and (4) are sufficient to solve for the five selenocentric orbital parameters in terms of the transfer-trajectory parameters. However, it is not convenient to solve the equations in this form because, in general, solutions exist for only a limited range of Ω_0. For example, if i_0 is 90° there are obviously values of Ω_0 such that the transfer-trajectory plane would not intersect the sphere of influence. To overcome this type of difficulty Ω_0 is eliminated from the equations by squaring and adding the second and third of equations (3) to give a new set of three equations.

$$\left(\dot{x}^2 + \dot{y}^2 + \dot{z}^2\right) - 2\mu_e\left(x^2 + y^2 + z^2\right)^{-1/2} - \frac{2\mu_e}{r_0}\left[\left(\frac{V}{V_p}\right)_0^2 - 1\right] = 0$$

$$\left(y\dot{z} - z\dot{y}\right)^2 + \left(z\dot{x} - x\dot{z}\right)^2 - 2\mu_e r_0\left(\frac{V}{V_p}\right)_0^2 \cos^2\gamma_0 \sin^2 i_0 = 0 \right\} \qquad (5)$$

$$\left(x\dot{y} - y\dot{x}\right) - \sqrt{2\mu_e r_0}\left(\frac{V}{V_p}\right)_0 \cos\gamma_0 \cos i_0 = 0$$

After a solution is found to these equations, the corresponding value of Ω_0 can be determined from equations (3) by substituting the solution on the right and solving for $\sin\Omega_0$ and $\cos\Omega_0$. The resulting value defines the injection time so that the vehicle will enter the sphere of influence at the desired point.

If the transfer-trajectory characteristics $\left(\left(\frac{V}{V_p}\right)_0, \ i_0, \ \gamma_0, \ r_0\right)$ and the periselenian distance R_p are specified, equations (4) and (5) define a relationship between any two of the selenocentric orbital parameters. In particular, since the geometrical characteristics of the selenocentric hyperbola and the resulting lunar orbit are of particular interest, it would seem advantageous to reduce the equations to a form which gives the selenocentric orbital inclination as a function of the selenocentric orbital nodal position. Obtaining such a relationship by algebraic manipulation is difficult and, in general, numerical techniques are required. Solutions of equations (4) and (5) can be generated by an iterative technique such as the Newton-Raphson method outlined in reference 4.

Some typical solutions of equations (4) and (5) are presented in figures 3 and 4 for the five transfer trajectories whose injection conditions are given in table I. Figure 3 presents the locus of entry points on the sphere of influence for each trajectory. Each point on the entry-point curve corresponds to a particular orbital plane as illustrated schematically in the figure. Also, three of the resulting orbital planes are indicated by dashed lines for each entry-point locus. The entry point for each orbital plane is indicated by a dot and the direction of orbital motion in the plane is given by the arrow.

8
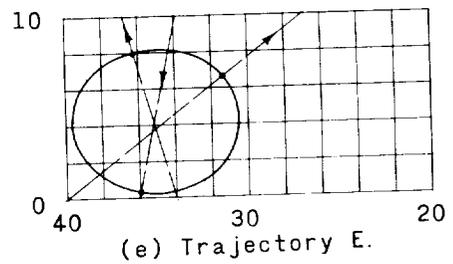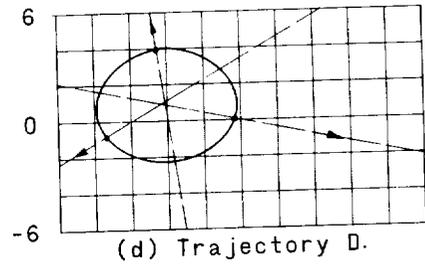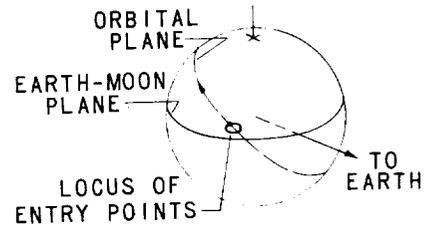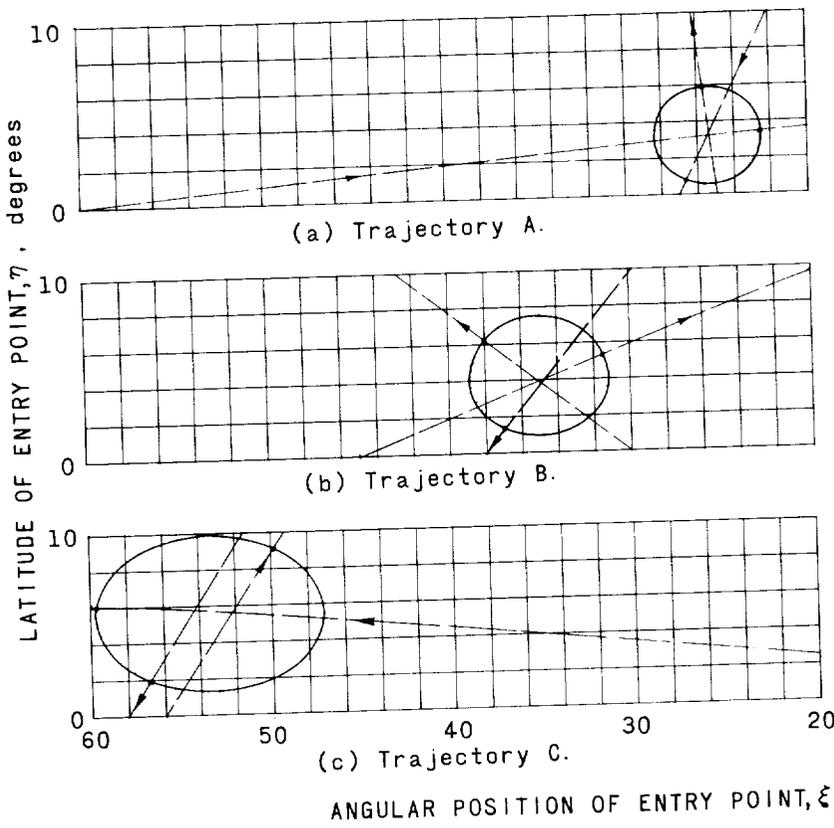
Figure 3.- Locus of entry points on sphere of influence.

TABLE I.- CHARACTERISTICS OF TRANSFER TRAJECTORIES

$$\left[\text{Geocentric injection radius} = 4,259 \text{ miles; injection angle} = 0\right]$$

| Trajectory	$\left(\dfrac{V}{V_p}\right)_o$	$i_o,$ deg	$R_p,$ miles	$\tau,$ hours
A	1.000	30	1,180	50
B	.995	30	1,180	62
C	.992	30	1,180	81
D	.995	5	1,180	62
E	.995	30	1,580	62
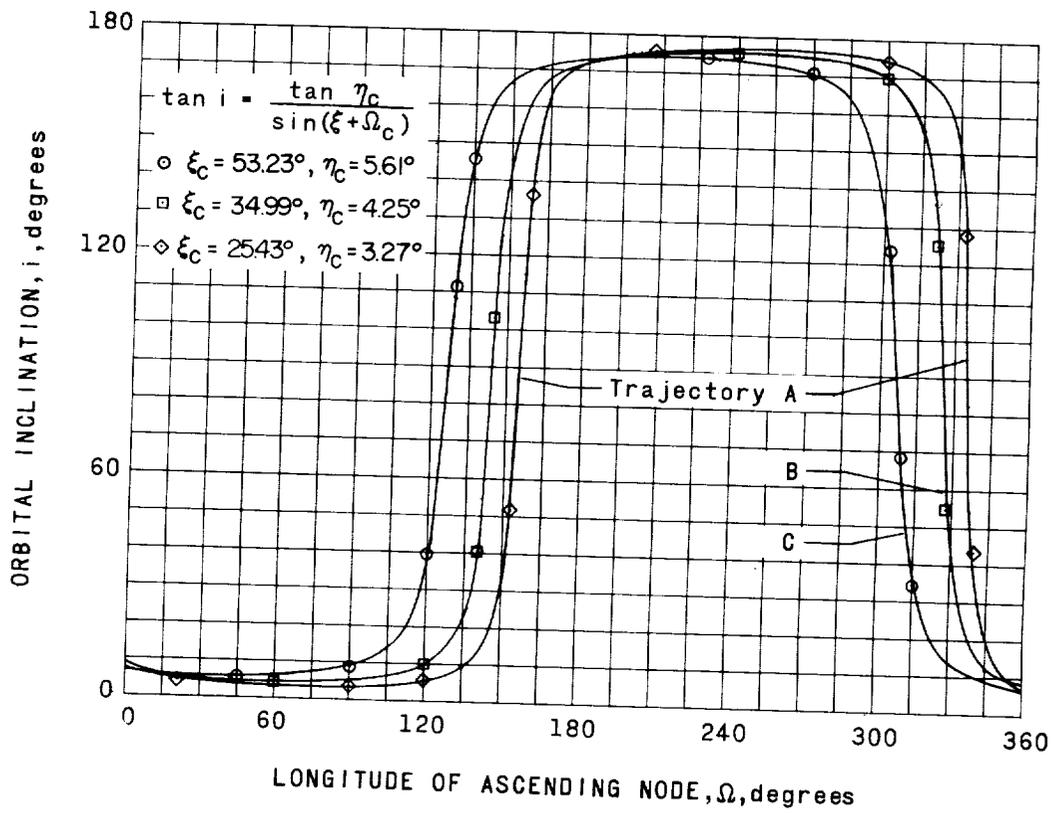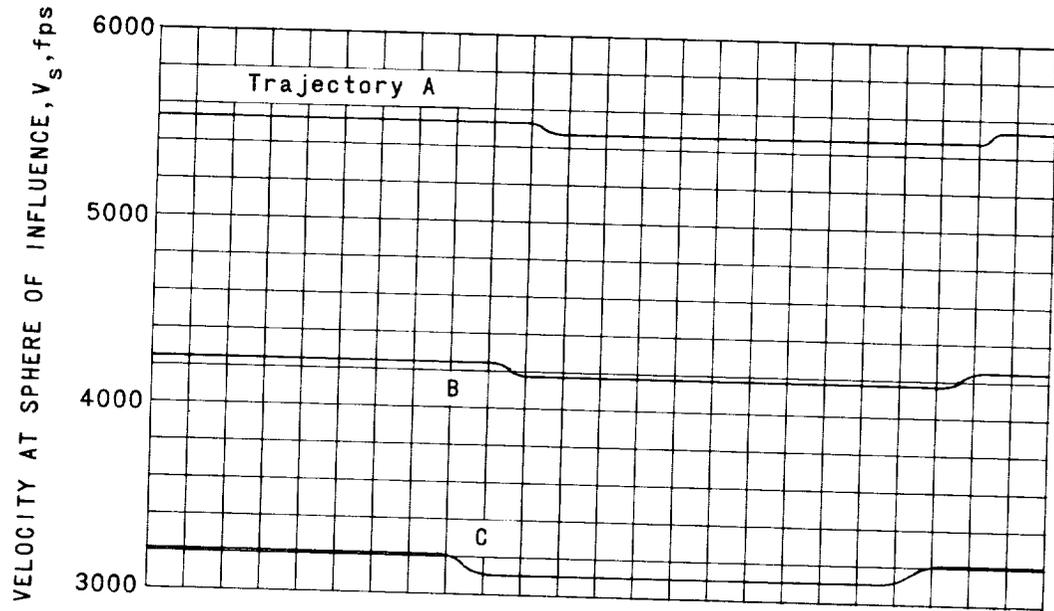
Figure 4.- Selenocentric orbital characteristics.

It is seen from figures 3(a), (b), and (c) that the entry-point curve for each trajectory is nearly circular and the curve becomes more circular and smaller as the transfer-trajectory energy increases. In addition, the center of the curve moves toward the earth-moon line and slightly toward the earth-moon plane as the energy increases. Comparing figure 3(b) with 3(d) indicates that decreasing the inclination does not change the size or shape of the curve but moves the center closer to the earth-moon plane. Finally, from figures 3(b) and 3(e) it is seen that increasing the periselenian distance of the approach hyperbola increases the size of the entry-point locus but does not displace the center appreciably.

It is to be noted that for the higher energy cases the orbital planes nearly pass through the center of the region bounded by the entry-point curve. If this were true for all the orbital planes, then the inclination and nodal position of the selenocentric orbital plane could be related by the laws of spherical trigonometry to give

$$\tan i \sin(\Omega + \xi_c) = \tan \eta_c \tag{6}$$

where ξ_c and η_c are the coordinates on the sphere of influence of the center of the entry-point region. The lower part of figure 4 shows a comparison between the inclination as a function of nodal position as calculated from equations (4) and (5) and as calculated from equation (6) by using the indicated values of ξ_c and η_c. The agreement for these three cases seems to indicate that equation (6) is a valid relation between the inclination and nodal position of the selenocentric orbital plane. Therefore, for a specific transfer trajectory, $\left(\gamma_o, \ r_o, \left(\frac{V}{V_p}\right)_o, \ i_o\right)$, equation (6) defines a relationship between Ω and i, and only one of these elements can be chosen arbitrarily. From the equation and from figure 5, it is seen that the nodal position can vary over the range $0°$ to $360°$ while the inclination is limited to the range $|\eta_c| \leqq i \leqq \{180 - |\eta_c|\}$. The highly inclined lunar orbits correspond to nodal positions near the entry-point region and low inclination orbits correspond to nodal positions nearly $90°$ away from the entry point.

These results might have been anticipated from the following reasoning. Suppose it is desired to calculate the entry-point locus for some transfer trajectory and some periselenian distance R_p. First, equations (5) are utilized to calculate the entry point for the selenocentric hyperbola which has zero angular momentum; i.e., impacts normal to the moon's surface and therefore $\beta = 0$. Let the location of this normal-impact entry point on the sphere of influence be denoted by the point (ξ_n, η_n). The solution of equations (5) also gives a value of V_s at the point (ξ_n, η_n). If this value of V_s is substituted into equation (4) along with the desired value of $R_p \neq 0$, a value of $\beta \neq 0$ can be calculated. For typical transfer trajectories and for R_p not much greater than the lunar radius, the value of $\beta < 5°$. Now consider a new or modified entry point (ξ, η)
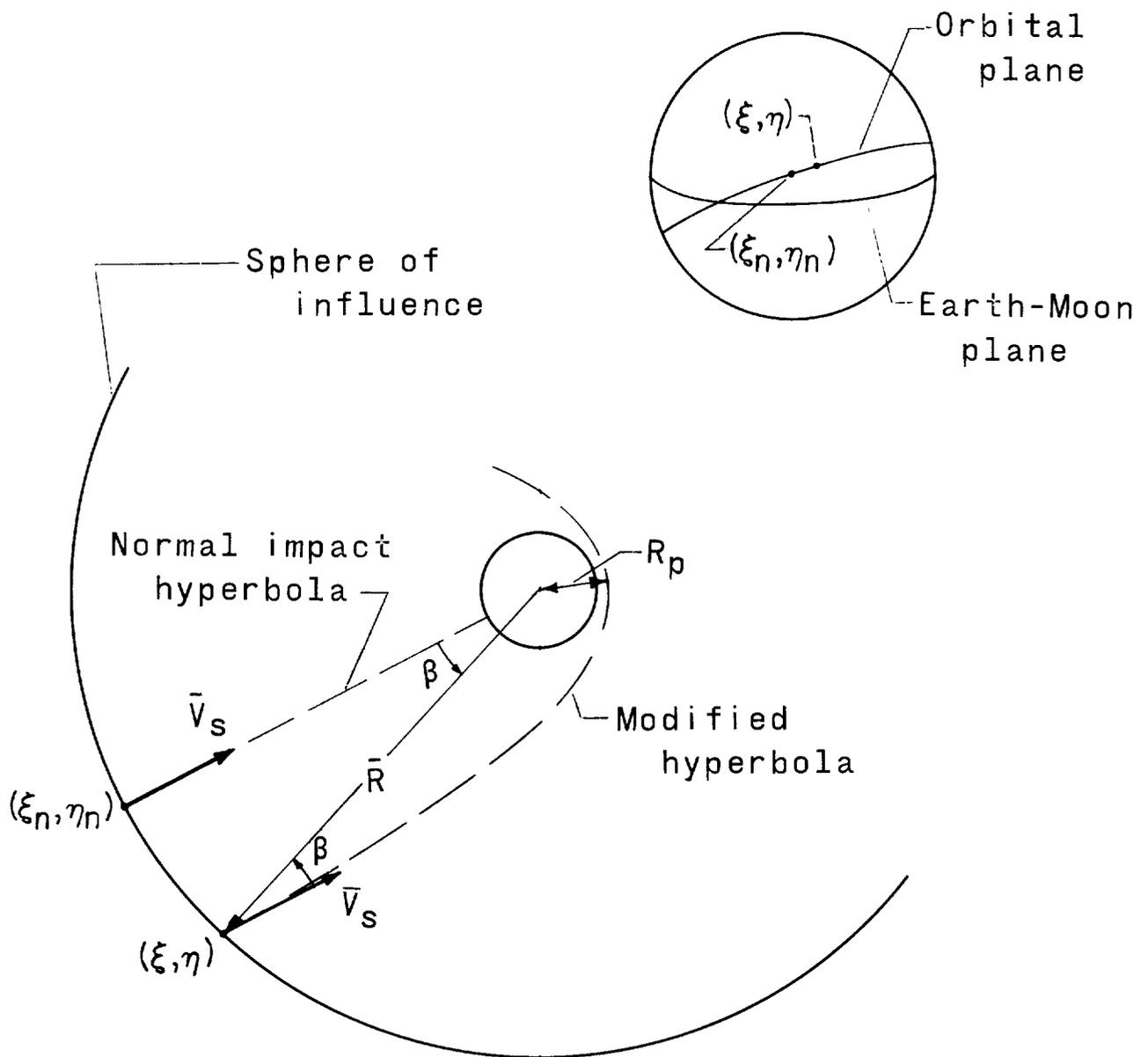
Figure 5.- Illustration of the modified selenocentric trajectory.

which is displaced β from the normal-impact entry point $\left(\xi_n, \eta_n\right)$. The situation is shown schematically in figure 5 where the plane of the paper represents the selenocentric plane connecting the two points $\left(\xi_n, \eta_n\right)$ and (ξ, η). In general, small changes in the injection time and Ω_0 can be made so that the vehicle passes through this modified entry point without changing any of the other characteristics of the normal-impact transfer trajectory. This displacement of less than 5° on the lunar sphere of influence represents a small change in position relative to the earth, hence the geocentric velocity vector of the vehicle at the point (ξ, η) will be nearly equal to the velocity vector if the vehicle entered at the point $\left(\xi_n, \eta_n\right)$. Consequently, the velocity of the vehicle relative to the moon

is nearly the same at the two points. By assuming the velocity vector at the two points to be equal, it is seen from the geometry of figure 5 that the angle between $\overline{V}_S$ and $\overline{R}$ at the modified entry point is also β; thus, the modified trajectory will have the desired periselenian distance. It is also seen that the plane connecting points (ξ_n, η_n) and (ξ, η) will be the plane of motion. The same arguments hold for any point which is displaced β from the normal-impact entry point. Hence for a given transfer trajectory and periselenian distance, the locus of entry points would be expected to approximate a circle with center at point (ξ_n, η_n) and all the orbital planes would be expected to pass through the center of this circle. Therefore the node and inclination of the resulting selenocentric orbits will be related by an equation analogous to equation (6) with ξ_c and η_c replaced by ξ_n and η_n, respectively,

$$\tan i \sin (\Omega + \xi_n) = \tan \eta_n \tag{7}$$

and the geometrical properties of the resulting lunar orbits will depend on the injection conditions $\left(\gamma_0, \quad r_0, \quad \left(\dfrac{V}{V_p} \right)_0, \quad i_0 \right)$ through the coordinates of the normal-impact entry point $\left(\xi_n, \eta_n \right)$. The next section presents a method for relating these entry-point locations to the injection conditions.

Approximate Equations and Solutions

The calculation of the normal-impact entry points can be readily obtained by using the laws of conservation of geocentric energy and angular momentum as before. For this case the selenocentric orbital parameters (i, Ω, θ) have no meaning; instead the coordinates (ξ, η) of the entry point will be used to specify the direction cosines. The normal-impact condition provides an additional piece of information; namely, that the velocity vector $\overline{V}_S$ must be parallel to $\overline{R}$ at the entry point. Hence

$$\overline{R} = R\left(l_1 \overline{e}_x + m_1 \overline{e}_y + n_1 \overline{e}_z \right)$$

$$\overline{R} = R\left(-\cos \eta \, \cos \xi \, \overline{e}_x + \cos \eta \, \sin \xi \, \overline{e}_y + \sin \eta \, \overline{e}_z \right)$$

and

$$\overline{V}_S = V_S\left(\cos \eta \, \cos \xi \, \overline{e}_x - \cos \eta \, \sin \xi \, \overline{e}_y - \sin \eta \, \overline{e}_z \right)$$

Substitution of $\overline{R}$ and $\overline{V}_S$ into equations (1) and (2) and then into (3) gives for the angular-momentum components:

$$h_x = h \sin i_o \sin \Omega_o = -RV_m \sin \eta$$

$$h_y = -h \sin i_o \cos \Omega_o = DV_s \sin \eta$$

$$h_z = h \cos i_o = -RV_m \cos \eta \cos \xi + DV_m - DV_s \cos \eta \sin \xi$$

(8)

Likewise equations (5) become

$$V_s{}^2 + V_m{}^2 - 2V_s V_m \cos \eta \sin \xi - 2\mu_e \left(R^2 + D^2 - 2RD \cos \eta \cos \xi\right)^{-1/2}$$

$$+ \frac{2\mu_e}{r_o}\left[1 - \left(\frac{V}{V_p}\right)_o^2\right] = 0$$

$$\left(R^2 V_m{}^2 + D^2 V_s{}^2\right)\sin^2\eta - 2\mu_e r_o \left(\frac{V}{V_p}\right)_o^2 \cos^2\gamma_o \sin^2 i_o = 0$$

(9)

$$RV_m \cos \eta \cos \xi + DV_s \cos \eta \sin \xi + \sqrt{2\mu_e r_o}\left(\frac{V}{V_p}\right)_o \cos \gamma_o \cos i_o - DV_m = 0$$

With the substitutions,

$$\lambda = \frac{V_s}{V_m} \qquad\qquad \alpha = \frac{R}{D}$$

$$\mu = \cos \eta \sin \xi \qquad\qquad \nu = \cos \eta \cos \xi$$

these equations take a form which is convenient for the application of a Newton-Raphson iteration for λ, μ, and ν

$$\lambda^2 - 2\mu\lambda - \left(\frac{2\mu_e}{dV_m{}^2}\right)\left(1 + \alpha^2 - 2\alpha\nu\right)^{-1/2} + \left(\frac{2\mu_e}{r_o V_m{}^2}\right)\left[1 - \left(\frac{V}{V_p}\right)_o^2\right] + 1 = 0$$

$$\left(\lambda^2 + \alpha^2\right)\left(1 - \mu^2 - \nu^2\right) - \left(\frac{h}{DV_m}\right)^2 \sin^2 i_o = 0$$

(10)

$$\mu\lambda + \alpha\nu + \left(\frac{h}{DV_m}\right)\cos i_o - 1 = 0$$

where as before $h = \sqrt{2\mu_e r_o}\left(\frac{V}{V_p}\right)_o \cos \gamma_o.$

14
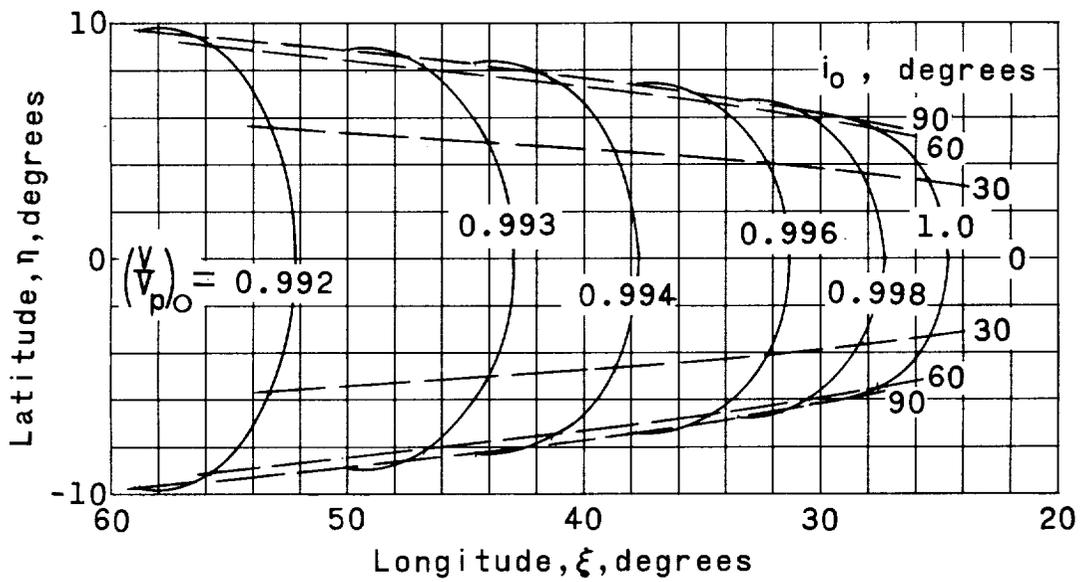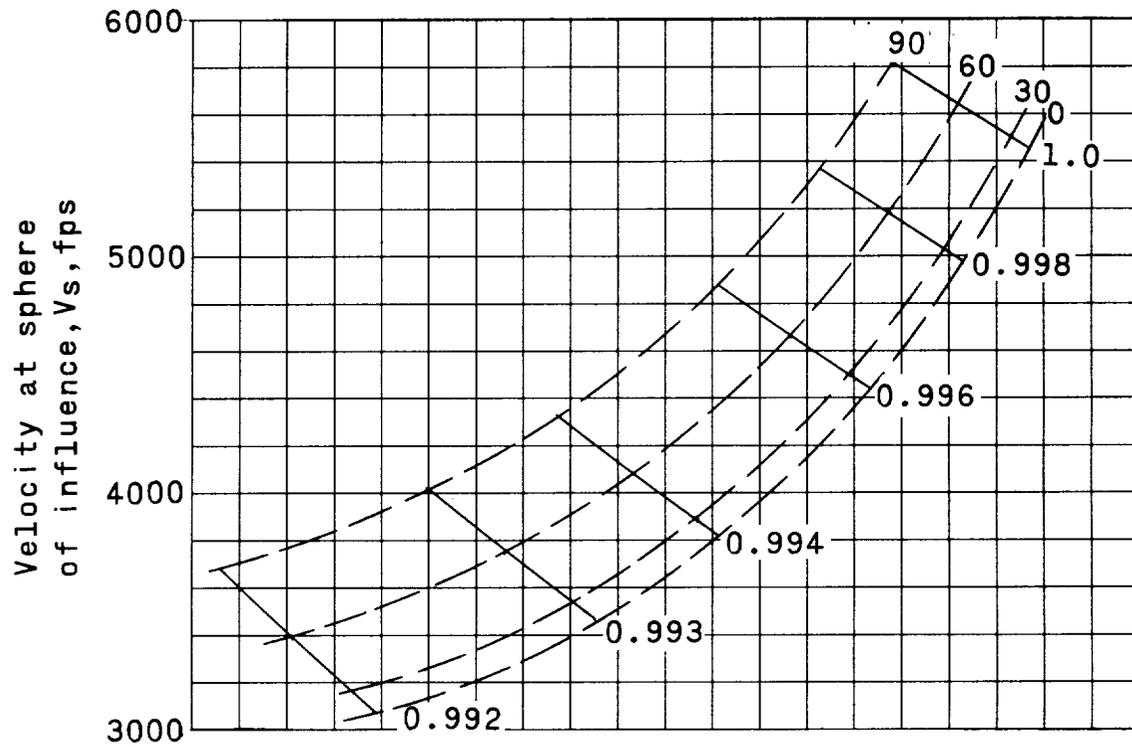
(a) $\gamma_0 = 0$.

Figure 6.- Location of normal-impact entry points on sphere of influence, $r_0 = 4,259$ miles.
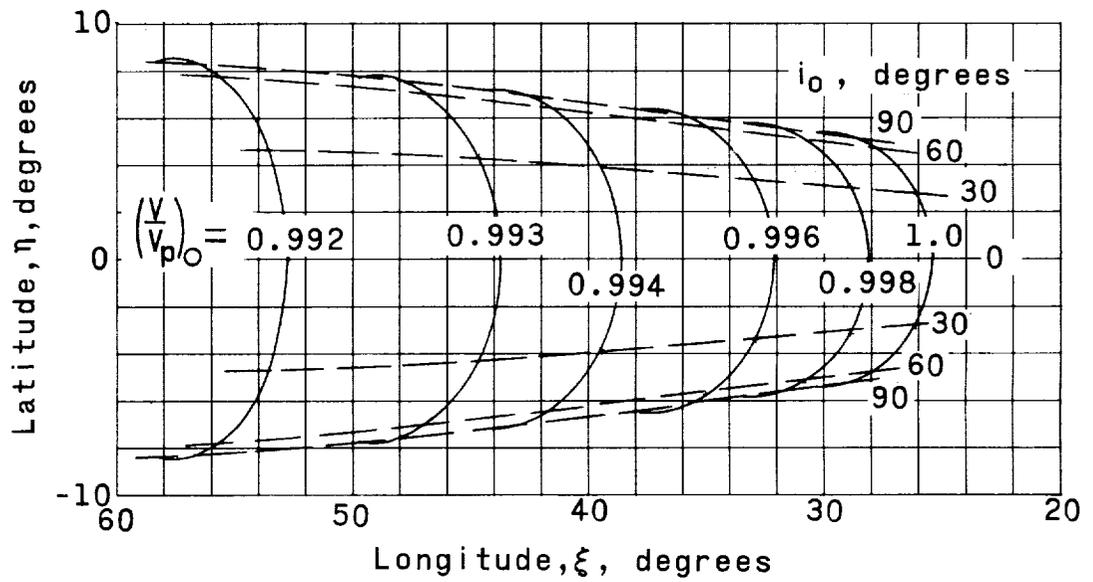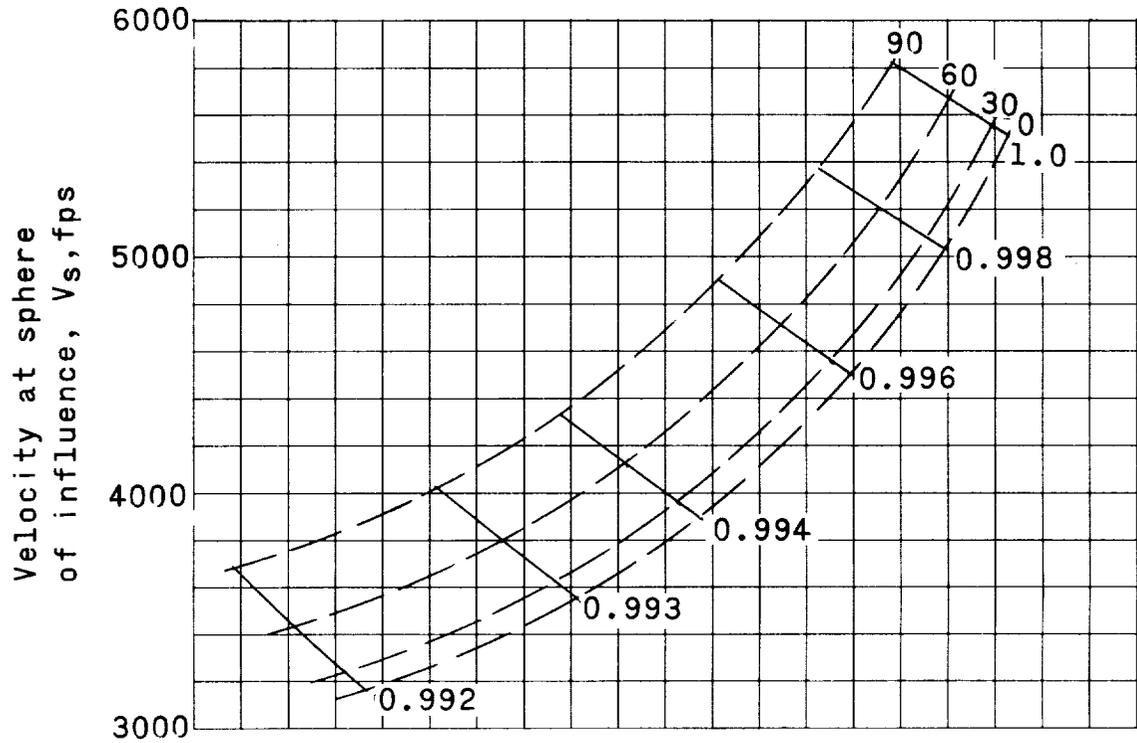
(b) $\gamma_0 = 30°$.

Figure 6.- Concluded.

Simultaneous solutions to equations (10) are presented in figure 6 for a range of injection-velocity ratios and transfer-trajectory inclinations and for two injection flight-path angles. The loci of entry points are symmetric about the earth-moon plane and, as can be deduced from the first two of equations (8), the solutions corresponding to $\eta < 0$ are for transfer trajectories for which the vehicle is ascending at the time of passage through the sphere of influence and those solutions corresponding to $\eta > 0$ are trajectories for which the vehicle is descending. A normal-entry point location from figure 6 is to be interpreted as representing the center of the entry-point locus for selenocentric trajectories which do not impact normally. The radius of the entry-point locus, β, is to be calculated from equation (4) by using the appropriate value of V_s from figure 6. With this interpretation the resulting entry-point loci will have the same properties as the loci obtained from the more exact calculations and presented in figure 3. Also note that the value of V_s at the normal-impact entry point agrees well with the more exact values presented at the top of figure 4.

For the range of velocities presented here the entry-point region is seen to represent a small area on the sphere of influence. This fact can lead to some serious limitations on the types of selenocentric orbits suitable for a given mission. For example, it is shown in reference 5 that for circumlunar trajectories the maximum allowable inclination of the selenocentric orbital plane is 17°. Hence, if such a fail-safe trajectory is to be utilized as the nominal lunar-approach trajectory for manned exploration missions, then the landing sites are restricted to a narrow band about the earth-moon plane. A similar example of such a restriction on the possible landing sites is afforded by assuming that the lunar orbit rendezvous technique is utilized for missions with exploration times of a few days. For this case the inclination of the selenocentric orbital plane must be a few degrees greater than the latitude of the desired landing site if an efficient recovery operation is to be possible during the entire exploration period. Under this condition it is clearly seen to be impossible to land at the midlatitudes (30° to 60°) on the western limb of the moon, for to be able to do so requires selenocentric orbital inclinations between approximately 30° to 60° and orbital nodal positions in the first and third quadrants. These latter requirements are incompatible with the fact that the limited entry-point area is in the second quadrant which demands that, for such high inclination selenocentric orbits, the nodal position must be in the second and fourth quadrants. A more quantitative description of the possible landing areas can be determined by using the data of figure 6 once the transfer-trajectory characteristics and the lunar-landing procedures have been specified.

For the normal impact case the calculation of the required nodal position for the transfer trajectory becomes a simple matter. Dividing the first two of equations (8) gives

$$\tan \Omega_O = \left(\frac{R}{D}\right)\left(\frac{V_m}{V_s}\right) \tag{11}$$

Over most of the injection-velocity range, V_s is approximately equal to or greater than V_m (3,361 fps) and hence

$$\tan \Omega \lesssim \alpha = 0.1498$$

Therefore, the nodal line for the earth-to-moon transfer trajectory must fall in the first and third quadrants and be within 10° of the earth-moon line at the time the vehicle enters the sphere of influence. Comparing the results of equation (11) with the more exact results from equations (4) and (5) showed good agreement except when the inclination of the transfer-trajectory plane became within a few degrees of 0° or 180°.

Another characteristic of the solution can be obtained from the second equation of (9) which can be written as

$$\sin \eta = \sqrt{\frac{2\mu_e r_0 \left(\frac{V}{V_p}\right)_0^2 \cos^2 \gamma_0}{R^2 V_m^2 + D^2 V_s^2}} \sin i_0 \tag{12}$$

Neglecting R^2 in comparison with D^2 and approximating μ_e/D by V_m^2 the equation can be closely approximated by

$$\sin \eta \approx \sqrt{\frac{2r_0}{D}} \left(\frac{V_m}{V_s}\right)\left(\frac{V}{V_p}\right)_0 \cos \gamma_0 \sin i_0 \tag{13}$$

In reference to figure 6, V_s is more strongly dependent on $\left(\frac{V}{V_p}\right)_0$ than on i_0, hence this relationship shows that for a transfer trajectory with a given energy and injection angle the sine of the latitude of the normal impact entry point is proportional to the sine of the transfer-trajectory inclination. But as shown previously, the minimum-inclination lunar orbit which can be established from a given transfer trajectory has an inclination equal to the latitude of the normal-impact entry point. Thus the preceding equation gives an approximate relationship between the minimum-inclination lunar orbit and the transfer-trajectory characteristics. Hence, if it is desirable to establish a lunar satellite in the earth-moon plane, i_{min} would represent the magnitude of the least orbital plane change that would be required. As an example, consider a transfer trajectory with an energy consistent with that for the close lunar approach circumlunar mission; that is, $\left(\frac{V}{V_p}\right)_0 \approx 0.9937$. Taking an average value of V_s from figure 6 of about 4,000 fps and substituting into equation (13) gives

$$(\sin i)_{min} \approx 0.16 \cos \gamma_0 \sin i_0$$

From a propulsion standpoint the most unfavorable conditions for getting into the earth-moon plane are $i_0 = 90^\circ$ and $\gamma_0 = 0$ which would result in a required plane change of at least 9°. The most favorable conditions are of course $i_0 = 0$ or the unrealistic condition $\gamma = 90^\circ$.

18

Once the normal-impact entry point is determined, the geometrical properties of all possible lunar orbits are given by equation (7),

$$\tan i = \frac{\tan \eta_n}{\sin(\Omega + \xi_n)}$$

The accuracy of this relation when η_n and ξ_n are taken from figure 6 is indicated in figure 4, for the values of ξ_c and η_c used there are actually the corresponding values of ξ_n and η_n. Notice that equation (7) does not depend explicitly on the periselenian distance of the approach hyperbola; however, the accuracy of equation (7) does depend on this parameter, for if R_p is large compared with the lunar radius, β will not be a small angle and the approximations required in deriving the equation will not be valid. Numerical comparisons with the more exact results from equations (4) and (5) for the median-energy transfer trajectory, $\left(\frac{V}{V_p}\right)_0 = 0.995$, indicate that for a given Ω, equation (7) will predict the resulting inclination within 3° for periselenian altitudes up to 500 miles. For values of Ω where i is not changing rapidly with Ω and for the same range of R_p, equation (7) predicts i to within 0.2°.

Before figure 6 can be utilized to determine η_n and ξ_n in equation (7), the injection conditions must be known. The injection-velocity ratio and flight-path angle are usually determined from launch vehicle considerations and are generally known within small tolerances. The inclination of the transfer-trajectory plane to the earth-moon plane is somewhat more arbitrary. Reference 6 presents a method for calculating the transfer-trajectory inclination as a function of the launch azimuth at Cape Canaveral and the coasting arc in the terrestial orbit.

CONCLUDING REMARKS

An analysis has been made of the geometrical characteristics of lunar orbits which can be established from typical earth-moon transfer trajectories. A patched-conic approximation was utilized and proved convenient for analyzing the general qualitative aspects of the problem.

The results of the study indicate that lunar orbits with a wide variety of geometrical characteristics can be established from essentially the same transfer trajectory; however, there is a minimum-inclination lunar orbit which can be established from any given transfer trajectory. An approximate relation shows that the sine of the minimum inclination is proportional to the product of the sine of the transfer-trajectory inclination to the earth-moon plane and the cosine of the injection flight-path angle of the transfer trajectory. For median-energy transfer trajectories, the most unfavorable situation results in a minimum inclination of about 9°.

In addition, it was shown that to a first approximation all the orbital planes have a common line of intersection. This results in a relation between the lunar orbital inclination and nodal position; hence, only one of these two parameters can be chosen arbitrarily. For the range of transfer-trajectory energies considered here, the locus of the common points of intersection of the selenocentric orbital planes represents a small area on the sphere of influence. This result can lead to the exclusion of the midlatitudes of the moon's western limb as possible landing sites if the lunar orbit rendezvous technique is utilized.

Langley Research Center,
    National Aeronautics and Space Administration,
        Langley Station, Hampton, Va., February 1, 1963.

REFERENCES

1. Gapcynski, J. P., and Tolson, R. H.: Trajectory Considerations for the Return to Earth Phase of Lunar Missions. [Preprint] 2487-62, American Rocket Soc., July 1962.

2. Plummer, H. C.: An Introductory Treatise on Dynamical Astronomy. Dover Pub., Inc., 1960.

3. Thomas, David F., and Bird, John D.: A Parametric Investigation of the Lunar Orbit Rendezvous Scheme. NASA TN D-1623, 1963.

4. Scarborough, James B.: Numerical Mathematical Analysis. Fourth ed., The Johns Hopkins Press (Baltimore), 1958.

5. Tolson, Robert H.: Maximum Latitude of Lunar Landing Sites. ARS Jour., vol. 32, no. 7, July 1962, pp. 1091-1092.

6. Tolson, Robert H.: Effects of Some Typical Geometrical Constraints on Lunar Trajectories. NASA TN D-938, 1961.